

CORROSION FATIGUE CRACKING OF STAINLESS STEELS IN CHLORIDE SOLUTIONS

H. Schmidt, B. Weiss, and R. Stickler +)

The corrosion fatigue resistance of several Mo-containing austenitic and ferritic-austenitic stainless steels under high-frequency (20 kHz) cyclic loading conditions was investigated in pure water and synthetic seawater. A statistical evaluation of the results was found essential for revealing the effects of environment and material's parameter on the fatigue life. A method of ranking the various steels according to their corrosion fatigue behavior is proposed. Fractographic observations indicate that fatigue crack initiation occurred under passive corrosion conditions along slip lines in the austenitic and at the interphase boundaries in the ferritic-austenitic steels.

INTRODUCTION

A wide variety of austenitic and ferritic-austenitic stainless steels with high Mo-contents have been developed which exhibit excellent corrosion resistance in chloride containing aqueous solutions. However, it is known that the corrosion behavior of such steels can be detrimentally affected by superimposed cyclic stresses (Schmidt et al (1), Speidel (7)). This corrosion affected fatigue, termed corrosion fatigue (CF), poses a considerable technological and economical problem.

Recent theoretical considerations of the corrosion fatigue phenomena by Müller (8,9) point out the pronounced influence of simultaneous corrosion and fatigue exposure on crack nucleation, with pitting corrosion and passive corrosion the most likely failure mechanisms in the case of stainless steels.

A thorough understanding of the CF-behavior of stainless steels and the effects of composition, pretreatment, microstructure, and environment requires a huge experimental effort, particularly in view of the statistical nature of fatigue failure processes. Prohibitive experimental times are required if the CF-resistance of material needs to be evaluated for low cyclic loading amplitudes up to high numbers of loading cycles.

A reduction of the experimental efforts appears feasible by an increase in test frequency as proposed by several investigators. A literature review is included in a publication by Schmidt et al (1), the state-of-the-art of high-frequency CF-testing is summarized in the proceedings of a recent conference (2). Comments on the frequency effect under CF-conditions can be found in reference (9) while experimental data over a wide range of test frequencies have been published for ferritic steels (7).

+) University of Vienna, Vienna, Austria.

Initial results about the CF-behaviour of several stainless steels in various aqueous solutions obtained by a 20 kHz resonance fatigue test method are included in reference (1). It was the objective of present investigation to provide experimental results suitable for a ranking of the CF-resistance of several newly developed stainless steels in pure water and in various concentrations of synthetic seawater. In view of the limited amounts of specimen materials available a testing procedure was adopted which was expected to permit a statistical evaluation of the test results. A fractographic investigation of all specimens was performed to yield information about deformation reactions, damage accumulation, fatigue crack initiation and propagation in the test solutions.

EXPERIMENTAL PROCEDURES

Test equipment. A detailed description of the experimental set-up has been published previously (1, 10). The mechanical resonance system that excites a suitably dimensioned specimen to longitudinal push-pull resonance vibrations at a test frequency of 20 kHz is shown schematically in Figure 1. The environmental chamber with the pumping circuitry (to provide a constant pressurized flow of the test liquid) is indicated. The entirely non-metallic corrosion test loop was purged with air, the temperature of the liquid was thermostatically controlled to 20 C.

The stresses occurring in the mid-section of the specimens were computed from strain values measured by means of strain gauges applied to this region. The required dynamic Young's modulus was determined for each specimen material by a resonance method at the same test frequency of 20 kHz.

The sensitivity of the automatic switch-off control was set to terminate the test when a fatigue crack had traversed approximately 25% of the cross section of the specimen, thus preventing excessive damage to the fatigue fracture surface.

Corrosion test liquids. The specimens were tested in pure (distilled) water or synthetic seawater (according to DIN 50900) in various concentrations (standard DIN, 0.1 and 2.5 DIN concentrations). For comparison specimens were also tested in 3%NaCl-water solutions buffered with lactic acid to pH = 5 as described by Weiss et al (10).

Specimen materials. The composition of the various evaluated steels is listed in Table 1, which also contains information about heat treatment, grain size, mechanical properties, and dynamic Young's modulus. All steels were tested in the heat treated condition with the exception of the cold-worked austenitic stainless steel which was tested in a cold-drawn condition to obtain maximum strength.

Specimen geometry. Depending on the dimensions of the starting materials (rolled or drawn rods) specimens were machined either with dumbbell geometries (diameter of gauge section 3 mm) or as cylindrical rods (4 or 5 mm diameter). The length of the specimens corresponded to 1/2 of the wavelength of longitudinal vibrations at the test frequency. The machined surfaces were mechanically and electrolytically polished to remove all machining surface damage.

Preliminary tests revealed that the rod-shaped specimens of the high-strength duplex steel and of the heavily cold-worked austenitic steel could not be cyclically strained at amplitudes sufficiently high to produce fatigue failure in pure water below 10^9 loading cycles. Since the dimensions of the starting material prevented the preparation of dumbbell specimens, a circular notch (tip radius 1.5 mm) was machined in the mid-section of each rod with

notch-depths to result in a stress concentration of $k_t = 1.56$ (for steel X3CrMnNiMoN25 6 4) and $k_t = 1.60$ (for steel X2CrNiMo18 12-CW). Willertz and Patterson (11) showed by finite element analysis that the notch factors computed for resonance specimens are in good agreement with those of statically loaded specimens. In view of the uncertainties related with a quantitative evaluation of the notch effect under fatigue conditions, however, only a relative comparison between the results obtained from notched specimens should be attempted.

Selection of cyclic stress amplitudes. In view of the of the limited amount of specimen material it was impossible to determine complete S-N curves for each steel. Fatigue testing had to be limited to only one or two cyclic stress amplitudes if statistically significant data points were to be collected for each stress level.

In order to facilitate a comparison between the results of the various steels, a cyclic stress amplitude of $0.5xR_m$ was initially aimed for since a linear relationship between the fatigue strength in air and the tensile strength was reported for a number of stainless steels by Müller (9). It was planned to test additional specimens at a lower stress level corresponding to a fatigue life in pure water of 10^9 loading cycles.

Differences between nominal R_m values for typical production melts and the actual values determined from the specimen materials caused a slight deviation from the envisaged σ_a/R_m ratio for some of the steels, as listed in Table 2.

The stress levels for the notched specimens were selected on the basis of a desired fatigue life between 10^6 and 10^8 loading cycles. The stresses were measured under identical operating conditions using plain specimens. The stresses in the root of the notch may be computed by a multiplication of the plain specimen stress with the listed stress concentration factors.

Table 1 - Composition and Mechanical Properties of Specimen Material

Alloy DIN	Composition, weight %					heat treat- ment +) C/min	ASTM grain size	Mechanical properties ++)				A %	dyn. Young's modulus N/mm ² 20kHz, 20C	
	Cr	Ni	Mo	Cu	Mn			Rp0,1 N/mm ²	Rp0,2 N/mm ²	Rp1,0 N/mm ²	Rm N/mm ²			
X2CrNiMo1810	17	12	2	-	1,3	-	1070/20	6	226	249	299	577	63	193 400
X2CrNiMo1812(CW)	18	15	3	-	1,7	-	deformed	-	1276	1397	1576	1614	5	189 000
X3CrNiMoN17135	17	14	5	-	1,4	0,17	1100/20	5,5	298	318	380	683	54	193 200
X2NiCrMoCu25205	20	26	4	1,3	0,9	-	1100/20	2	221	236	283	599	61	193 200
X2CrNiMoCuN1716	17	16	6	1,5	1,2	0,15	1150/15	0,5	359	384	446	702	48	186 400
AISI 316 L	18	11	2	-	1,7	-	1090/60	3	-	340	-	620	40	193 400
X4CrNiMo217	21	8	3	1,4	0,9	-	1050/20	10	357	389	457	686	40	224 000
														duplex
X3CrMnNiMoN2564	25	4	2	-	6	0,4	1050/20	8	808	832	900	986	26	197 400
														duplex

+) followed by water quench ++) mean values of 2-4 tests of miniature tensile specimens machined from the shoulders of fatigue test specimens

EXPERIMENTAL RESULTSFatigue Data

The experimentally determined numbers of loading cycles to failure are plotted in Figures 2 to 8 for the various steels in the form of failure-probability versus loading-cycle diagrams. The failure probability p was calculated according to Maennig and Pfender (12) by the following relationship:

$$p = i/(n+1).$$

Using this method of data presentation distinct differences between the results of steels tested in pure water and in the 2.5DIN seawater could be revealed. The influence of test frequency can be deduced from Figure 3 which contains results obtained at a test frequency of 200 Hz by Zitter (3). These tests were carried out at 20 C and $R = -1$ with specimens prepared from the identical material as provided for the 20 kHz experiments. Although a considerable effect of the test frequency on the fatigue life can be noticed, the trend in the influence of the environment appears comparable for both test frequencies. As shown by Karner (5) for one of the steels, the reduction in fatigue life at 20 kHz is similar for 2.5DIN and DIN seawater, whereas failure in 0.1DIN seawater occurs inbetween the fatigue life in pure water and the concentrated solutions.

The increase in fatigue life by a decrease in the cyclic stress amplitude can be seen for the highly alloyed austenitic steel in Figure 4. The difference in fatigue life of specimens tested in pure water to that of specimens tested in 2.5DIN seawater increases with decreasing stress amplitudes. A similar effect can also be deduced from Figure 7 for the duplex steel, in this case the lower stress amplitude appears to coincide with the fatigue limit in pure water.

In most of these diagrams the straight line relationship of the data points indicates a statistical distribution of the failure. Deviations from such a straight line relationship are noticed for the steels which were tested in form of notched specimens, Figure 7 and 8. This deviation might be related to unavoidable variations in the notch dimensions.

From the diagrams in Figures 2 to 8 it is possible to deduce values for the number of loading cycles corresponding to a failure probability of 50%. These $N_{f,p=50\%}$ -values may be considered as sensitive indicators of the influence of the testing environment on fatigue life. As shown in Figure 7, a minor difference in fatigue life between 2.5DIN seawater and the 3%NaCl solution is expressed in a distinct difference in this parameter, Table 2. A pronounced reduction of the fatigue life of the cold worked austenitic steel in the 3%NaCl solution is apparent in Figure 8.

The test results are summarized in Table 2 in which data by Weiss (4) for solution treated AISI type 316L tested at 20 kHz in an 'inert' environment (transformer oil) have been included. As already mentioned before, the data obtained from notched specimens should only be used for a relative comparison.

Fractographic Evaluation

Detailed examination of the specimen surface near the fatigue crack region and of the fracture surfaces were carried out by light and scanning electron microscopy. In the following only a brief summary of the findings can be given.

Table 2 - Summary of Test Results

Alloy DIN	σ_{a2} N/mm ²	$\sigma_a/R_{p0,2}$	σ_a/R_m	N_f for p=50% in environment at 20 C			Cyclic Frequency	Ref. *
				2.5DIN seawater	Others	Pure water		
X2CrNiMo1810	271	1,09	0,47	1.0x10 ⁶		3.8x10 ⁶	20 kHz	1
AISI 316 L	271	0,80	0,44		4.5x10 ⁶ in oil		20 kHz	4
	251	0,73	0,40		5.0x10 ⁷ in oil		20 kHz	4
X3CrNiMoN17135	236	0,74	0,35	3.4x10 ⁶		4.8x10 ⁷	20 kHz	1
	150	0,47	0,22	2.1x10 ⁶	6.1x10 ⁶ in 0,1 DIN seawater		200 Hz	3
	203	0,63	0,30	7.5x10 ⁵	2x10 ⁶ in 0.1 DIN seawater		200 Hz	3
	222	0,69	0,33	3.0x10 ⁶ (also in DIN sea- water)	8.2x10 ⁶ in 0.1 DIN seawater		20 kHz	5
X2NiCrMoCu25205	236	1,00	0,39	5.4x10 ⁶			20 kHz	1
X2CrNiMoCuN1716	363	0,95	0,52	2.5x10 ⁷		5.4x10 ⁷	20 kHz	
	304	0,79	0,43	5.5x10 ⁷		3.0x10 ⁸	20 kHz	
X4CrNiMo217	345	0,89	0,50	8.3x10 ⁵		4.7x10 ⁶	20 kHz	
X2CrNiMo1812(CW)	252+)		0,16++)		9.5x10 ⁶ in 3% NaCl-H ₂ O, pH=5	1.0x10 ⁹	20 kHz	2
X3CrMnNiMoN2564	174+)		0,18++)	4.4x10 ⁷	3.6x10 ⁷ in 3% NaCl-H ₂ O, pH=5	10 ⁹	20 kHz	
	217+)		0,22++)	6.5x10 ⁶		2.0x10 ⁷	20 kHz	

+) Measured for plain specimens ++) Calculated for plain specimens, actual specimens contained notch with $k_t=1.56$ (for X3CrMnNiMoN2564) and $k_t=1.60$ (for X2CrNiMo1812-CW)

Specimens of the steels with the lowest alloying content, i.e. steel X2CrNiMo18 10 and the comparable steel AISI type 316L exhibited a high density of fine slip lines in the vicinity of the fatigue crack. On the specimens tested in 2.5DIN seawater a marked etching attack could be noticed along some of these slip lines and around inclusions, forming sharp transgranular trenches and grooves, respectively. In each case only a single crack nucleation site could be identified on the fracture surface, consisting of a planar transgranular crystallographic fracture which extended over several grains. The fatigue crack zone consisted of transgranular ductile fracture with fatigue striations. On the fracture surfaces of specimens tested in 2.5DIN seawater these striations appeared on a coarser scale, in addition islands of grain boundary failure could be recognized. The fracture surface of the specimen tested in oil exhibited a much smaller transgranular crystallographic nucleation zone and a pronounced transgranular ductile fracture with fine striations. No characteristic features in addition to a single nucleation site could be resolved on the fracture surfaces of the cold-worked steel X2CrNiMo18 12-CW tested in either environment.

On the surfaces of the specimens of the higher alloyed steels tested in pure water no slip traces could be observed although crack nucleation occurred obviously along crystallographic directions. In contrast, occasional slip traces could be found on the specimens tested in 2.5DIN seawater, probably indicative of a slight etching attack. In all cases the crack nucleation region consisted of crystallographic planes extending over several grains, with some signs of etching attack in the specimens tested in 2.5DIN seawater. The fatigue crack region consisted of a transgranular ductile fracture with occasional crystallographic steps. The specimens tested in 2.5DIN seawater exhibited a

mixed transgranular/intergranular fracture mode with pronounced secondary cracking and etching attack along some of the crystallographic facets.

On the surfaces of the duplex steels X4CrNiMo21 7 and X3CrMnNiMoN25 6 4 (of very fine grain size) no slip traces could be detected. Crack nucleation appears to have occurred along interphase boundaries. Fatigue exposure in 2.5DIN seawater caused a slight etching attack of one of the phases and a marked delineation of the interphase boundaries. Specimens tested in pure water contained only one crack nucleation site while several crack nuclei could be identified in the specimens tested in 2.5 DIN seawater. The fatigue cracks propagated during exposure in pure water by a mixed transgranular-ductile/interphase-boundary process. The rougher appearance of the fatigue fracture surface of specimens tested in 2.5DIN seawater could be related to a transgranular-crystallographic/interphase-boundary failure. In the specimens fatigue exposed in 3%NaCl-water solutions at pH=5 the interphase-boundary separation appeared as the predominant fracture mode.

CONCLUSIONS

1. The described test procedure (20 kHz resonance fatigue test method) was found capable of revealing effects of environments (e.g. pure water and concentrated seawater) on the fatigue life of highly alloyed stainless steels.
2. Due to the statistical nature of fatigue failure, test results may scatter over a broad range. In this case statistical consideration must be applied in the design of the test program in order to facilitate a better differentiation of the experimental data. Since at least 8 data points are considered to be required for a statistical evaluation (12) a sufficient number of specimens must be tested for each experimental condition (e.g. stress amplitude, environment). If only a limited amount of specimen material is available the selection of the proper stress amplitudes poses some problems. As a guideline a value of the cyclic stress amplitude to be selected about one half of the tensile strength may be useful (8). However, from the experience gained during this investigation it appears advisable to perform preliminary tests in order to obtain information on the approximate shape of the S-N curve in the range of loading cycles and environments envisaged. With the aid of this information the stress levels for detailed testing can be selected properly.
3. Comparison of the 20 kHz results with a limited amount of data of 200 Hz tests performed under otherwise comparable conditions revealed similar trends in the effects of environment on fatigue life, however, at much lower stress levels. In considering the frequency effect as discussed by several authors (7,9) the turbulent stirring action near the specimen surface under the 20 kHz cyclic loading should be taken into account (ultrasonic cleaning action, influence on the rate of chemical surface reactions).
4. The microscopic examination indicates that during fatigue exposure of the steels in 2.5DIN seawater a marked attack occurs along slip lines in austenitic steels, while in the duplex steels the interphase boundaries are noticeably attacked. It appears that this preferential etching causes an acceleration of crack initiation in 2.5DIN seawater as compared to pure water. The initiation of fatigue cracks in the saline environment appears to take place under passive corrosion conditions, with slip steps of sufficient height destroying locally the passivating surface layer, as proposed by Müller (9).
5. Although the observed corrosion fatigue behavior appeared significantly different, a relative ranking of the various steels on the basis of the limited amount of test data proved to be difficult in view of the differences in stress levels and corrosion effects. A method for a relative ranking of the

- various steels is suggested in Figures 9 and 10 in which the values of $N_{f,p=50\%}$ (as listed in Table 2) are plotted as function of a 'normalized cyclic stress amplitude' (σ_a/R_m). From the data in Figure 9 one may conclude that all fatigue tests have been conducted at stress levels above the fatigue limit of the steels in pure water. In the range of loading cycles between 10^5 and 10^9 the 2.5DIN seawater leads to a significant deterioration of the fatigue life. Steel X2CrNiMoCuN17 16 exhibits the highest fatigue strength of all the steels, as well in pure water as in the 2.5DIN seawater. The fatigue data for steels X2CrNiMo18 10 and X3CrNiMo17 13 5 seem to fall within one S-N band. The fatigue strength of steel AISI 316L tested in oil coincides fairly well with the results of the comparable steel X2CrNiMo18 10 at the higher stress level, the apparently superior fatigue life at the lower stress level may be interpreted as an indication of a mild CF-effect in pure water. The CF-resistance of the steel X2NiCrMoCu25 20 5 and of the duplex steel X4CrNiMo21 7 appears superior to that of the steels X2CrNiMo18 10 and X3CrNiMo17 13 5. A similar comparison for the high-strength steels tested in form of notched specimens, Figure 10, indicates that the duplex steel X3CrMnNiMoN25 6 4 is less sensitive to corrosion fatigue failure in 2.5DIN seawater and 3%NaCl-water solution at pH=5 than the steel X2CrNiMo18 12 in the cold worked condition.
6. The results obtained by accelerated testing at 20 kHz demonstrate that this test method is suited to provide a rapid screening and ranking of the CF-resistance of stainless steels in the selected solutions. Qualitative information on the effects of variations in alloy composition, pretreatment, and environmental chemistry can be collected in a short time. The test results may immediately be applicable to practical cases where components are exposed in comparable environments to high-frequency low-amplitude cyclic loading. Further experimental work is required to arrive at a quantitative relationship with corrosion fatigue results obtained at conventional test frequencies.

SYMBOLS USED

- i = sequential number of failed specimen in a ranking according to the number of cycles to failure
- n = total number of specimens tested at one stress level
- N = number of loading cycles
- $N_{f,p=50\%}$ = number of loading cycles to obtain failure with 50% fracture probability
- R = stress ratio (minimum stress/maximum stress)
- a = alternating stress amplitude

ACKNOWLEDGEMENTS

This investigation was partly funded by a grant from the Austrian Ministry of Science and Research. The specimen material was kindly supplied by VEW-Ternitz. The authors thank Prof. H. Zitter (MUL-Leoben) for helpful advises and Dr. H. Kohl (VEW) for numerous critical discussions. The assistance of Mr. F. Bauer (VEW) in providing the tensile test data and of Drs. Müllner and Hessler for the determination of the dynamic Young's moduli is gratefully acknowledged.

REFERENCES

1. Schmidt H., Karner W., Weiss B., and Stickler R., 1981, Arab.J.Sci.&Eng.6, 197.
2. Proceedings of the First International Conference "Fatigue and Corrosion Fatigue up to Ultrasonic Frequencies", 1981, Champion, USA, J. Wells Ed., in print.
3. Zitter H., 1978, "Corrosion of Steels and Al-Alloys", SGAE Report No. A001, ME-147/78, 53.
4. Weiss B., 1978, "Determination of Fatigue Data for Metallic Materials", Final Report 78-IB-WF-B1.
5. Karner W., PhD-Thesis University of Vienna, 1979.
6. Kohl H., Rabensteiner G., Hochörtler G., 1980, Conference Proceedings "Alloys for the 80s", Ann Arbor, USA, paper 27.
7. Speidel M.O., 1980, Conference Proceedings "International Conference on Fracture, ICF-5", Cannes.
8. Müller M., 1981, BBC-Report KLR 81-66C, CH.
9. Müller M., 1982, Met.Trans. A13, 649.
10. Weiss B., Stickler R., Schider S., Schmidt H., 1981, "Corrosion Fatigue Testing of Implant Materials", in Reference 2, in print.
11. Willertz L.E., and Patterson L., 1981, "Finite Element Analysis of Stress Distribution around Notches in Resonance Specimens", in Reference 2, in print.
12. Maennig W., and Pfender M., 1976, Eng. Fract. Mech.8, 39.

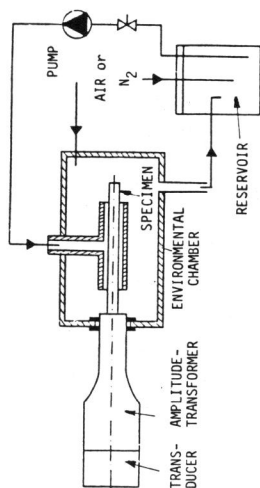


Figure 1 Experimental equipment (schematic)

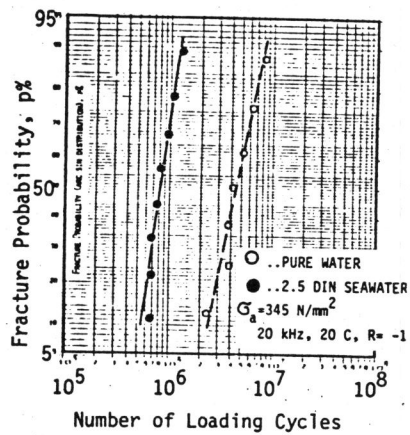


Figure 2 p-N diagram for steel X2CrNiMo18 10

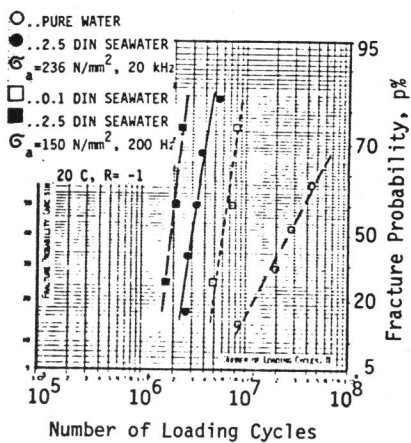


Figure 3 p-N diagram for steel X2CrNiMoN17 13 5

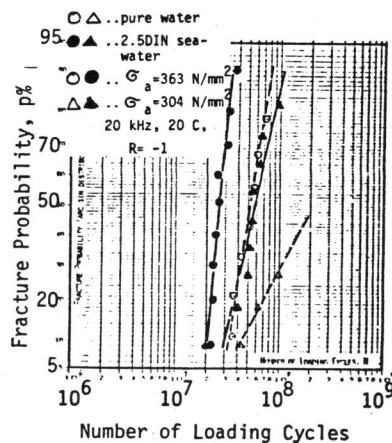


Figure 4 p-N diagram for steel X2CrNiMoCuN17 16

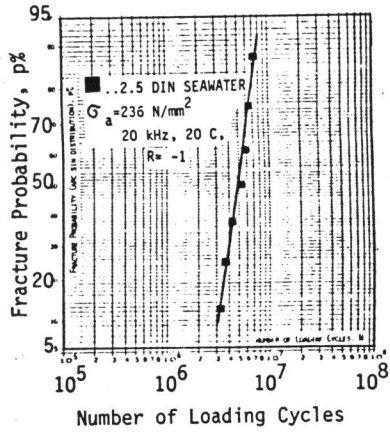


Figure 5 p-N diagram for steel X2NiCrMoCu25 20 5

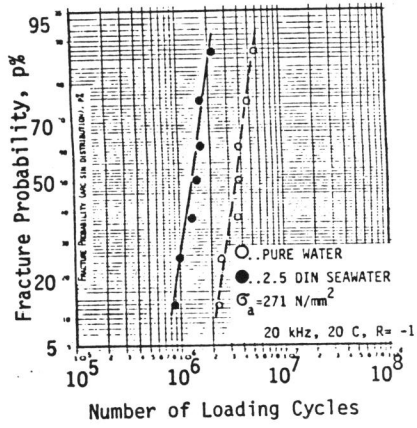


Figure 6 p-N diagram for duplex steel X4CrNiMoCu21 7

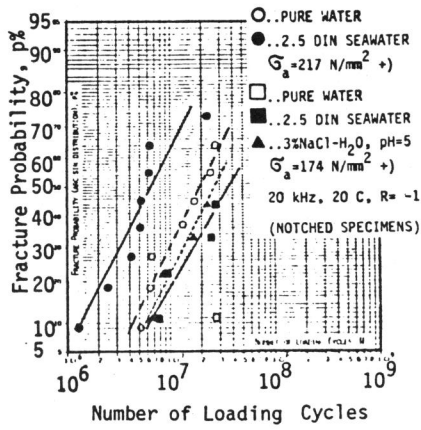


Figure 7 p-N diagram for duplex steel X3CrMnNiMoN25 6 4 (notched)

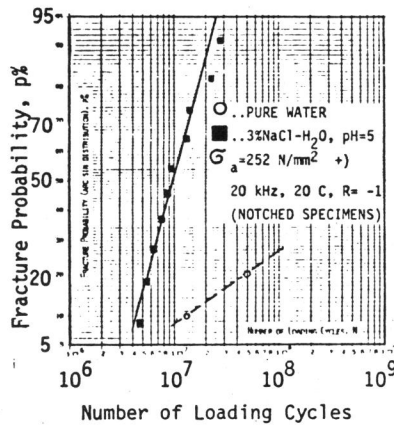


Figure 8 p-N diagram for cold-worked steel X2CrNiMo18 12 (notched)

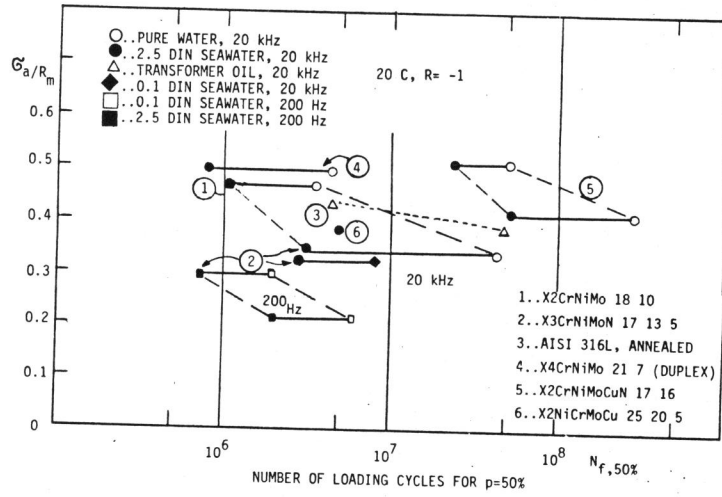


Figure 9 Summary of experimental results for steels tested as plain specimens

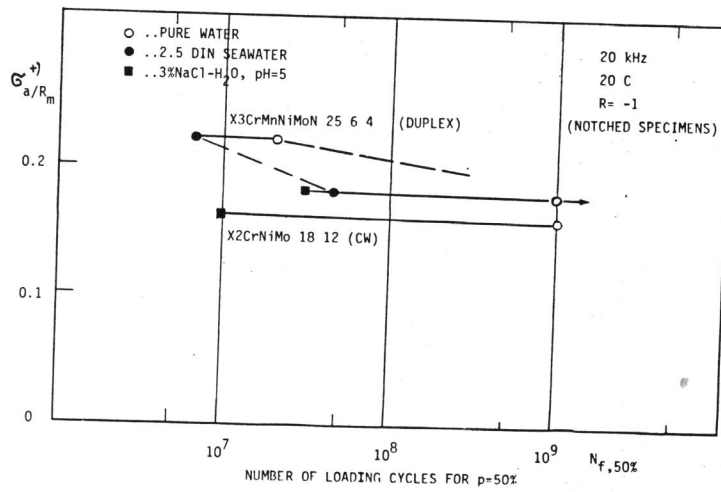


Figure 10 Summary of experimental results for steels tested as notched specimens